IRAQI Academic Scientific Journals
Iraqi Journal of Civil Engineering
Available online at https://www.iasj.net/
Journal homepage: https://www.iasj.net/iasj?func=issues&jId=141&uiLanguage=en

Studying the Effects of Negative Skin Friction on Single Piles in Basrah Governorate

Jasim M. Al-Battat[1], Prof. Haider S. Al-Jubair[2], Majid Faissal Jassim[3], Jawad K. Mures[4]

[1]*Department of Civil Engineering, College of Engineering, University of Basrah, Basrah-, Iraq*

[2]*Department of Civil Engineering, College of Engineering, University of Basrah, Basrah-, Iraq*

[3]*Department of Civil Engineering, College of Engineering, University of Al-Maaqal, Basrah-, Iraq*

[4]*Directorate of Municipality of Islah, Dhi-Qar, Iraq*

ARTICLE INFO

Article history:
Received 26 /03/ 2022.
Received in revised form 14/ 06/ 2022
Accepted 18 /06/ 2022
Available online 30 /07/ 2022

Keywords:
Finite element modeling,
Negative skin friction,
Single piles,
Pile Cross-Section,
Interface Effect,
Fill Height Effect.

ABSTRACT

The finite element method capable of simulating the behavior of deep foundations subjected to negative skin friction in Basrah soil is investigated. Single piles under drag forces are analyzed using the PLAXIS program with an axisymmetric model. Linear elastic, Soft Soil and Mohr-Coulomb constitutive relations are adopted, where higher order triangular element is chosen for pile and soil clusters. Both pile and soil are modeled using (15)-node triangular elements. Three sites in Basrah province (Umm Qasr Port, Khor Al-Zubair, and Shatt AlArab Hotel) were selected to perform this study. The soil profile and layer characteristics are obtained from the soil investigation reports. Where the negative skin friction is evaluated due to filling loads.

It is Conclusion that Small relative displacements are necessary to activate the negative skin friction. The elastic shorting for pile effect negative skin friction, due to increase relative displacement. The elastic shorting of the driven pile is more than that of the bored pile due to the less cross-sectional area of the driven pile. The results revealed proportional relation between the developed drag forces and pile section dimensions, interface friction factor, and fill height, with a maximum effect on the section dimension and minimum effect on the interface factor. The locations of neutral points are not sensitive to the above-mentioned factors.

DOI: **10.37650/ijce.2022.172883**

1. Introduction

Skin friction is developed on a pile shaft due to the relative vertical displacement between the pile under imposed loads and the surrounding soil. Thus, along pile length where the settlement of pile (ρ_{pile}) is less than the settlement of the surrounding soil (ρ_{soil}), the developing skin frictions will have an opposite sign (negative skin friction), compared to skin friction at the lower part of a pile. Thus, instead of contributing to pile resistance, the friction along the upper part of piles will add to the external loads, Fig. 1 (Kouretzis, G. 2018).

Ground settlement relative to the pile may be attributed to the following reasons (Bowles, J. 1997):

1. Weight of superimposed fill. Place a cohesive fill over a cohesionless soil deposit, so that pile is pushed downward as the fill consolidates. When a cohesionless fill is placed over a compressible cohesive deposit, there is some down drag in the fill zone, but the principal down drag will occur in the consolidated zone.
2. Groundwater lowering.

* *Corresponding author*. Tel.: 9647707337851;
E-mail address: jasimmohsinyasir@gmail.com

3. Disturbance of clay is caused by pile driving (particularly large displacement piles in sensitive clays), leading to the reconsolidation of the disturbed clay under its weight.

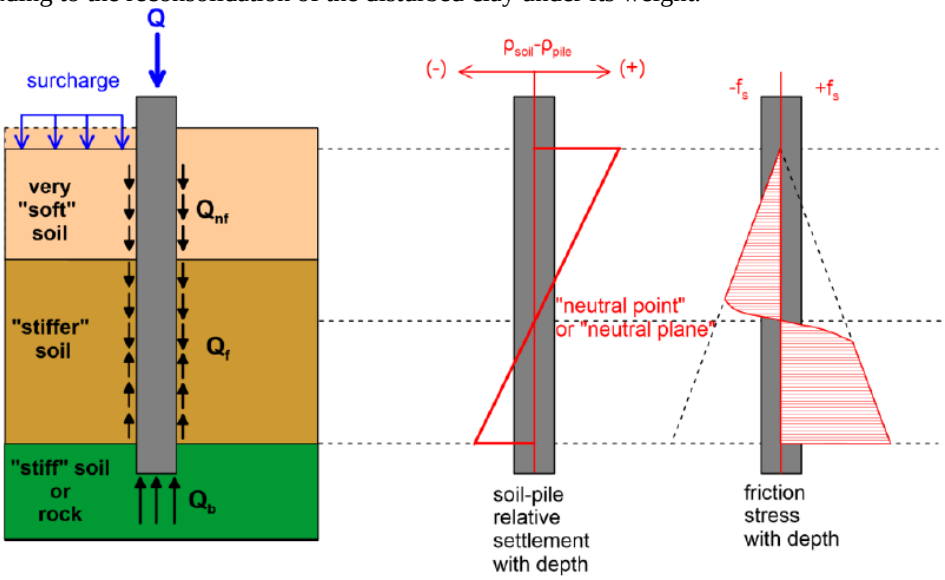

Fig. 1 Pile-soil relative displacement and friction stress distribution with depth (Kouretzis, G. 2018).

For negative skin friction to develop significantly, the pile should be fixed against vertical displacement. This condition is fulfilled when the pile point rests on bedrock or in a dense sandy layer.

It is common in Basrah Governorate-Iraq, to backfill the proposed project sites to raise their elevations and/or facilitate the accessibility of heavy equipment to them, before executing pile foundations that penetrate soft cohesive soil and rest in dense sandy soil. These results in applying additional forces on piles due to the consolidation of neighboring soil under the effect of fill load, since the pile construction process follows the backfilling process in a short period. The main objective of the present study is to evaluate the negative skin friction on piles penetrating Basrah soils utilizing Nonlinear two-dimensional finite element modeling. The approach is as follows:

1. Select three backfilled project sites and provide their in-situ soil characteristics.
2. Performing the analyses for the soft soil consolidation under fill load to determine the piles' negative skin stresses, the associated drag forces, and the influence distances within pile lengths.
3. Performing an extensive parametric study to investigate the effects of pile type; cross-sectional dimension; interface factor; and fill height, on the drag forces.

Zhang Investigated the time effect on negative skin friction for a super-long pile embedded in silt. An experimental program was conducted on a model pile where the soil surface was preloaded. The study revealed the considerable effect of time on drag force and the position of a neutral point. It was noted that, as the consolidation settlement proceeded, the negative skin friction value increased and then stabilized. The neutral point moved down and then stabilized, also (Zhang et al. 2014).

Abd El-Naiem conducted a laboratory experimental program on twenty-one pile models penetrating natural soft clay, and soft clay improved with stone columns, to study the distribution of skin friction on single piles during the consolidation of the surrounding soil under a uniform surcharge of (10 kPa). It was realized that the pile's axial strain distribution reflected the excess pore water pressure dissipation with time. Stone columns worked as vertical drains in accelerating the consolidation process, reducing the surrounding soil settlement, and increasing the pile capacity. It was also found that the bearing layer stiffness had a considerable effect on the position of the neutral plane (Abd El-Naiem et al. 2015).

Drbe utilized the finite element method via Plaxis-2D to investigate negative skin friction on driven concrete piles and to study the effects of pile length and pile load on the location of the neutral plane. The numerical solution was first evaluated against the measurements taken during model tests conducted by Indraratna et al. (1992). The capability of the finite element method in simulating the behavior of piles subject to negative skin friction was assessed. A value of (β = 0.2) was suggested by the authors to estimate the negative skin friction but, they recommended adopting a more reliable depth-dependent value. It was concluded that the neutral plane depth was proportional to the pile length. The results revealed decreased negative skin friction and neutral point depth, due to pile vertical load increase (Drbe et al. 2016). Siegel and Lucarelli developed a numerical model of a hypothetical pile and soil system to establish a theory regarding the development of negative skin friction on all piles. The finite difference-based software (FLAC-3D) was utilized to perform the numerical analyses. It was realized that

very small soil settlements were adequate to activate skin resistance. Consistent with the results of long-term monitoring, it was demonstrated that negative skin friction was developed in all piles due to soil settlement coupled with installation effects, consolidation under the sustained (head) load, and/or any other causes (Siegel and Lucarelli 2017).
Dey and Koch investigated the effect of pile driving on the position of the neutral plane. The updated Lagrangian formulation was used in the finite element package (ABAQUS) for modeling the pile driving process. The study was established on the case study of Indraratna et al. (1992). It was demonstrated that pile driving had a significant effect on the magnitude of negative skin friction. A considerable radial pore water pressure gradient was noted along pile length when pile driving was considered. Higher negative skin friction values were obtained for the first type of analysis. The first type of analysis revealed higher stiffness at the pile base, less settlement of the pile tip, and a deeper neutral plane (Dey and Koch 2017).

2. Finite element analysis

Two-dimensional finite element modeling to simulate the behavior of single piles is considered in this study. The discretized coupled Biot equilibrium and continuity equations in two dimensions are expressed as (Smith I. and Griffiths D. 2004):

$$[k_m]\{u\}+[c]\{u_w\}=\{f\},$$

$$[c]^T\left\{\frac{du}{dt}\right\}-[k_c]\{u_w\}=\{0\} \quad (1)$$

where, {u}, {u_w}, and {f} are the nodal displacement, excess pore water pressure, and external loading vectors, respectively; [k_m] and [k_c] are the stiffness and fluid conductivity matrices, respectively; and [c] is a rectangular coupling matrix consisting of terms of the form

$$\iint \frac{\partial N_i}{\partial x} N_j .dx.dy \quad (2)$$

where the N_i terms are the shape functions.

In this analysis, the PLAXIS finite element method software has been used for analysis. The boundary conditions are generated using the standard fixities in the PLAXIS software by defining prescribed displacements equal to zero at the line of symmetry and restricting nodal lateral translational movement at the domain sides, and both horizontal and vertical movements at the bottom of the domain. The axisymmetric model's boundary conditions have been used for modeling a single pile embedded into the soil.
Higher order triangular element is chosen for pile and soil clusters. Both pile and soil are modeled using (15)-node triangular elements providing fourth order interpolation for displacement (Brinkgreve, R.B.J. 2002).

3. Verification of the Program

3.1. Problem-I

This problem is drawn from Kiprotich (2015) where, the finite element method was used to study the documented behavior of a model bored pile, subjected to negative skin friction due to groundwater lowering, during centrifugal testing. The measured soil and pile properties are listed in Tables (1 and 2). The measured and calculated settlement profiles for soil and pile are illustrated in Fig. 2 (Kiprotich,N. 2015).

Table 1- The silty clayey soil and interface properties (problem-I).

Depth (m)	e_o	γ_{dry} (kN/m^3)	γ_{sat} (kN/m^3)	C_c	C_s	POP (kPa)	ϕ' (^{o})	δ (^{o})	Su/σ'_v	k (m/d)	ν_{ur}
22.5	1.4	11	17	0.15	0.036	117	32	25.8	0.32	0.00864	0.12

Table 2- Pile properties (problem-I).

Diameter (m)	Length (m)	E(kPa)	γ(kN/m^3)	ν
1.5	22.5	50e6	24	0.3

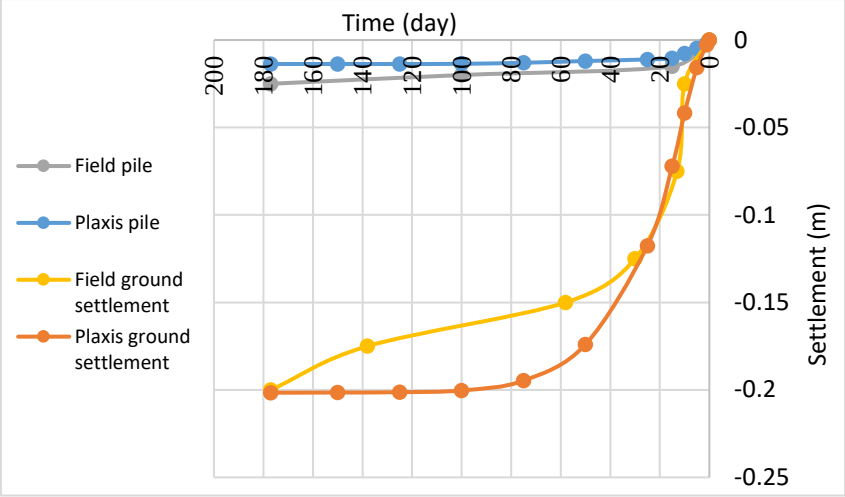

Fig. 2 Measured and calculated ground and pile settlement profiles with time (problem-1).

3.2. Problem-II

This problem is drawn from Belinchon et al. (2016), who studied a real case study via the finite element method. Uncoated and coated (0.25 m x 0.25 m) precast reinforced concrete piles were subjected to drag forces due to surface surcharge loading. The first loading scenario included the application of (0.8 m)-thick fill around piles after installation.

A (9.75 m)-long pile with a tip elevation of (8.75m) below soft clay ground level is analyzed where the original square cross-section of the pile is converted to an equivalent circular cross-section with a radius of (0.16 m) and the same perimeter of (1 m). The adopted soil and pile characteristics are listed in Tables (3 and 4), respectively. The pile is assumed vertically restrained at the top and modeled with a fixed-end anchor element (Belinchon et al. 2016). The variation of measured and calculated final settlement, with depth, is shown in Fig. 3.

Table 3- Initial stratification and soil parameters (problem-II).

Parameter	Fill	Soft clay	Sand
$Y_{max.}$(m)	0	-1	-10.5
$Y_{min.}$(m)	-1	-10.5	-15
Material modal	MC	Soft soil	MC
Drainage type	D	D	D
γ (kN/m^3)	18	14	16
E' (kN/m^2)	10000		30000
ν'	0.25		0.30
c' (kN/m^2)	6	2	1
ϕ'(^{0})	25	25	35
ψ (^{0})	0	0	5
λ*		0.1013	
k*		0.0231	
Pre-overburden pressure POP (kN/m^2)		15	

Table 4- Pile parameters (problem-II).

Parameter	Pile
Material modal	Linear
Drainage type	Non-porous
γ (kN/m^3)	24
E (kN/m^2)	26
ν	0.2

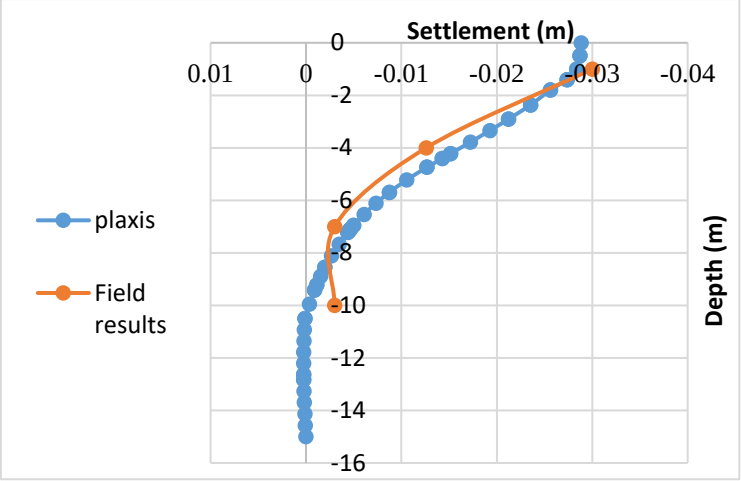

Fig. 3 Settlement profiles (problem-II).

4. IN-Situ Soil Stratigraphy and Properties

Three sites are selected for the study, namely: Umm-Qasr Port, Khor Al-Zubair, and Shatt Al-Arab Hotel [Fig. 4]. Soil and pile properties are listed in Tables (5 to 9). Where the water level is 3.2m, 3.5m, and 3m from the ground surface for Umm-Qasr Port, Khor Al-Zubair, and Shatt Al-Arab Hotel respectively.

Fig. 4 The selected site locations in Basrah city-Iraq.

Table 5- Soil properties at Umm Qasr Port (Fugro Middle East 2017).

Material	Fill	Medium stiff 1	Medium stiff 2	Dense/very dense sand
Depth of layer (m)	3 – 0	0 – -7.5	-7.5 – -14.5	-14.5 – -20
Material model	Mohr-C	SSM	SSM	Mohr-C
Drainage type	Drained	Drained	Drained	Drained
Unit weight, γ, γ_{sat} (kN/m^3)	18, 20.3	16, 18	16, 18	18.6, 20.4
Initial void ratio, e_{init}	0.5	0.85	0.85	0.4
Stiffness modulus, E (MPa)	48	3.5	2.5	57.6
Effective cohesion, c'(kPa)	1	3	3	1
Effective friction angle, $\phi'(^0)$	36	27	31	40
Dilatancy angle, $\psi(^0)$	6	0	1	10
Permeability, k (m/day)	4.32	0.00086	0.00086	4.32
Poissons ratio, v	0.27	0.4	0.4	0.3
Compression index (Cc)		0.25	0.25	
Recompression index (Cr)		0.03	0.03	

Table 6- Soil properties at Khor Al-Zubair site (Petrolinvest 2015).

Material	Fill	Loose silty sand	Medium stiff clay	Very stiff clay	Very dense sand
Depth of layer (m)	3 – 0	0 – -1	-1 – -10	-10 – -17	-17 – -25
Material model	Mohr-C	Mohr-C	SSM	SSM	Mohr-C
Drainage type	Drained	Drained	Drained	Drained	Drained
Unit weight, γ- γ_{sat} (kN/m^3)	18-20.3	16.5-20	15.6-19.4	15.6-19.4	19.4-21.5
Initial void ratio, e_{init}	0.5		0.61	0.61	
Stiffness modulus, E (MPa)	48	11.7	30	62.7	60
Effective cohesion, c'(kPa)	1	1	5	14.7	1
Effective friction angle, $\phi'(^0)$	36	31.8	23	20	40
Dilatancy angle, $\psi(^0)$	6	2	0	0	10
Permeability, k (m/day)	4.32	1	0.001	0.001	4.32
Poissons ratio, v	0.27	0.20	0.30	0.24	0.30
Compression index (Cc)			0.2	0.2	
Recompression index (Cr)			0.027	0.027	

Table 7- Soil properties at Shatt Al-Arab Hotel (University of Basra, Engineering Consulting Bureau 2012).

Material	Fill	Very stiff slit	Medium stiff slit	M. stiff slit	D. / V.D sand
Thickness (m)	3 – 0	0 – -1.5	-1.5 – -22	-22 – -25	-25 – -30
Material model	Mohr-C	Mohr-C	SSM	Mohr-C	Mohr-C
Drainage type	Drained	Drained	Drained	Drained	Drained
Unit weight, γ, γ_{sat} (kN/m^3)	18, 20.3	15.9, 18.9	14.7, 19.3	15.7,19	19.9, 22.7
Initial void ratio, e_{init}			0.89		
Stiffness modulus, E (MPa)	48	12.8	4.4	6.8	60
Effective cohesion, c'(kPa)	1	12	2.8	5	1
Effective friction angle, $\phi'(^0)$	36	24.5	26	24	40
Dilatancy angle, $\psi(^0)$	6	0	0	0	10
Permeability, k (m/day)	4.32	0.002	0.002	0.002	4.32
Poissons ratio, v	0.27	0.3	0.34	0.34	0.27
Compression index (Cc)			0.19		
Recompression index (Cr)			0.022		

Table 8- Interface strength, R_{inter}

Site	Interface strength, R_{inter}				
Umm-Qasr Port	Fill 0.7	Medium stiff 1 0.7	Medium stiff 2 0.7	Dense/v. D. sand 0.7	
Khor Al-Zubair	Fill 0.64	Loose silty sand 0.65	Medium stiff clay 0.81	Very stiff clay 0.85	V. dense sand 0.66
Shatt Al-Arab Hotel	Fill 0.64	Very stiff slit 0.82	Medium stiff slit 0.67	M. stiff slit 0.82	D. / V.D sand 0.66

Modulus elasticity can be calculated from (E = 4700$\sqrt{fc'}$) (ACI 318R-14), for bored pile (fc' =28 Mpa) and (fc' =40 Mpa) for driven pile.

Table 9- Adopted pile properties (ACI 318R-14).

Site	Pile type	Section dimensions (m)	Tip penetration below ground surface (m)	Modulus of Elasticity (MPa)	Poissons ratio
Umm-Qasr Port	Driven	0.285 x 0.285	16	29700	0.2
	Bored	0.8 dia.	16.5	24870	0.2
Khor Al-Zubair	Driven	0.285 x 0.285	11.5	29700	0.2
	Bored	0.8 dia.	12	24870	0.2
Shatt Al-Arab Hotel	Driven	0.285 x 0.285	26.5	29700	0.2
	Bored	0.8 dia.	27	24870	0.2

5. Analyses and Results

A non-linear two-dimensional finite element program is utilized to perform the analyses. The square pile sections are transformed into equivalent circular sections of similar perimeters. Soft Soil and Mohr-Coulomb yield criterion are used to represent the constitutive soil relations, whereas the pile material is treated as linear elastic. A typical discretization mesh is shown in Fig. 5.

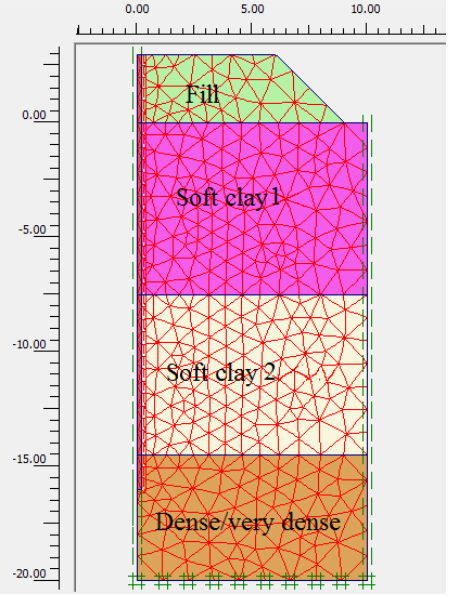

Fig. 5 Typical discretized mesh.

5.1. Umm-Qasr Port

The variation of soil surface settlement with time at Umm Qasr Port is shown in Fig. 6. The settlement ceased after around one year.

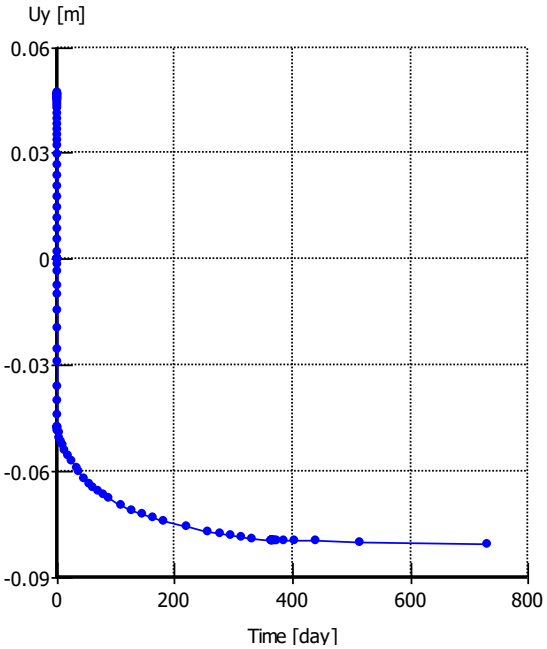

Fig. 6 Soil surface settlement vs. time at Umm-Qasr Port.

The comparisons between the vertical displacement of ground and both pile types (after 365 days) are shown in Figs. (7 and 8).

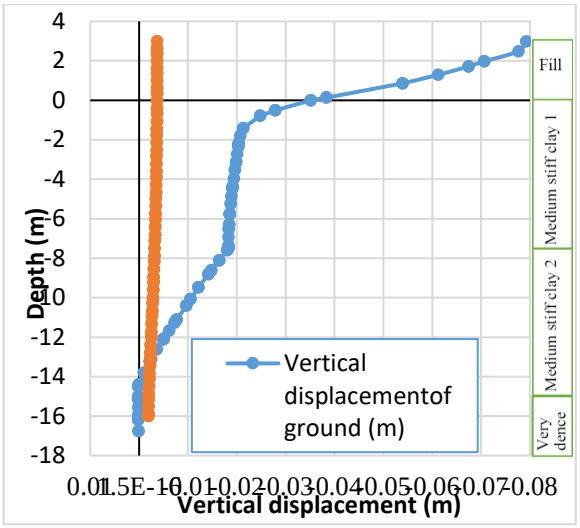

Fig. 7 Comparison between the vertical displacement of the ground and a single driven pile at Umm-Qasr Port.

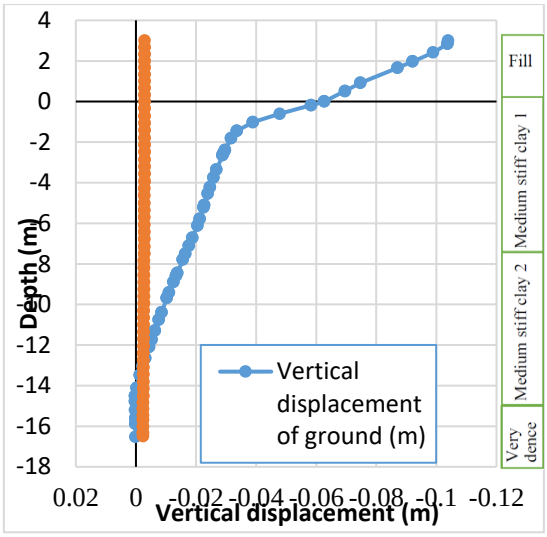

Fig. 8 Comparison between the vertical displacement of the ground and a single bored pile at Umm-Qasr Port.

It is apparent from Figs. (7 and 8) that, the settlement values of the ground surface (after 365 days) are (0.038 m) and (0.063 m) and their counterparts of driven and bored piles are (0.004 m) and (0.003 m), respectively. The relative displacements between soil and piles are (0.034m) and (0.060m). These relative displacements developed negative skin friction. The settlement values at pile butts (0.0037 m and 0.0029 m) are more than their counterparts at tips (0.0019 m and 0.0024) due to elastic shorting. The elastic shorting of the driven pile is more than that of the bored pile due to the less cross-sectional area of the driven pile.

The variations of skin stress with depth (after 365 days) for driven and bored piles at Umm-Qasr Port are shown in Figs. (9 and 10).

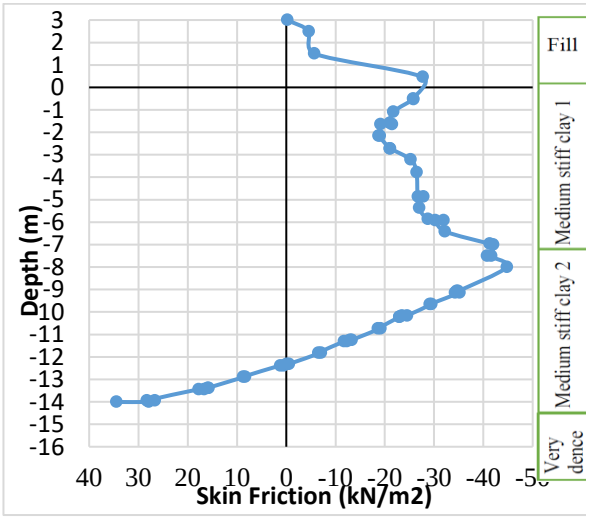

Fig. 9 Skin stress vs. depth for a driven pile at Umm-Qasr Port.

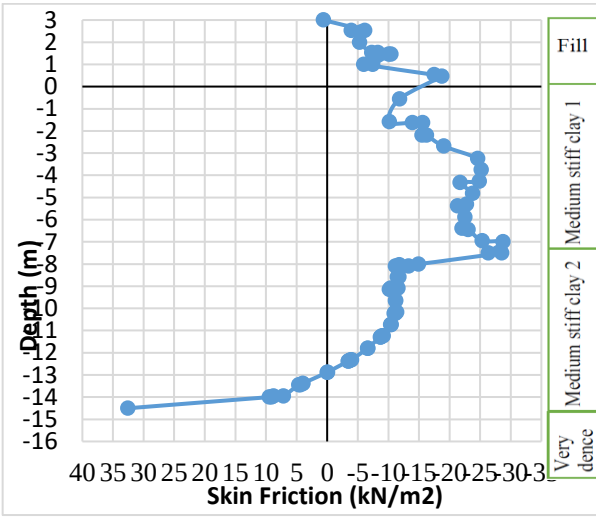

Fig. 10 Skin stress vs. depth for a bored pile at Umm-Qasr Port.

It is obvious from Figs. (9 and 10) that, the maximum negative skin friction is (44.8 kN/m^2) and (28.7kN/m^2), the neutral points (neutral points: the level where pile settlement equals settlement of the surrounding ground, Kouretzis, G. 2018) is at (12.4 m) and (12.9 m) from the ground surface, for the driven and bored piles, respectively.

5.2. Khor Al-Zubair

The time-soil surface settlement curve at Khor Al-Zubair is shown in Fig. 11. The settlement is ceased after around one year.

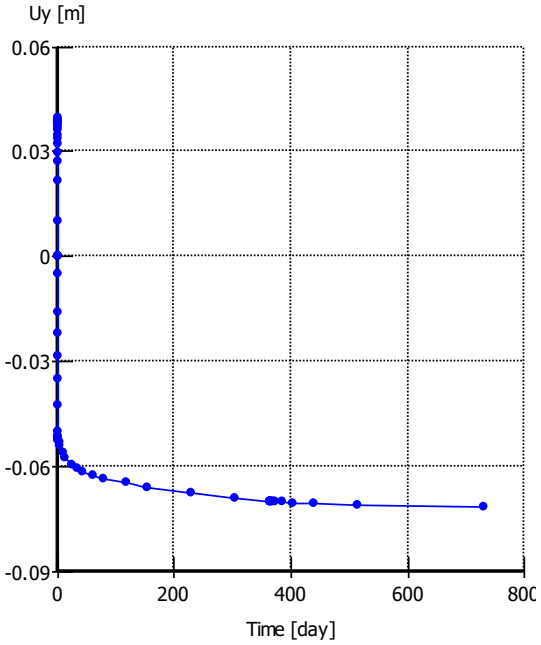

Fig. 11 Soil surface settlement vs. time at Khor Al-Zubair.

The comparisons between the vertical displacement of ground and both pile types (after 365 days) are shown in Figs. (12 and 13).

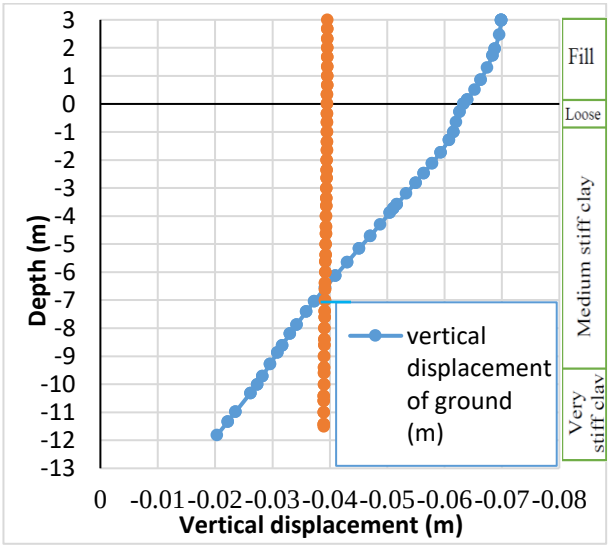

Fig. 12 Comparison between the vertical displacement of the ground and a single driven pile at Khor Al-Zubair.

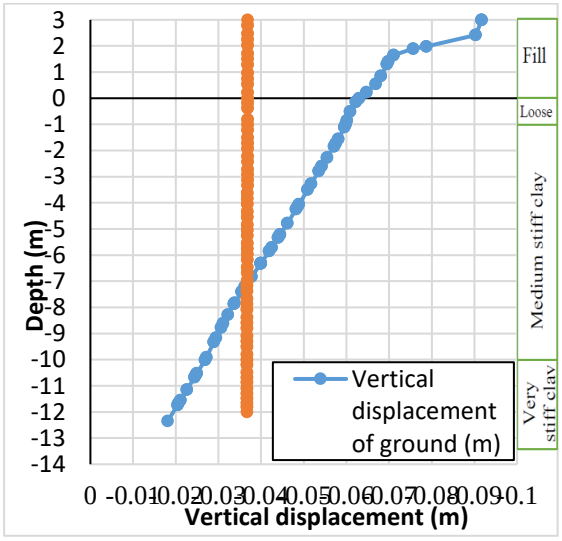

Fig. 13 Comparison between the vertical displacement of the ground and a single bored pile at Khor Al-Zubair Site

Figs. (12 and 13) show that, the settlement values of the ground surface (after 365 days) are (0.064 m) and (0.063 m), and the maximum settlement values of piles at the same time are (0.040 m) and (0.037 m) for driven and bored piles, respectively. The relative displacement values are (0.024m) and (0.026 m). In this site, higher pile settlement values are obtained because piles are resting in a cohesive bearing layer. The elastic shorting values of piles are low compared to other sites due to the reduced pile lengths.

The distributions of skin friction along pile shafts for driven and bored piles (after 365 days) are shown in Figs. (14 and 15).

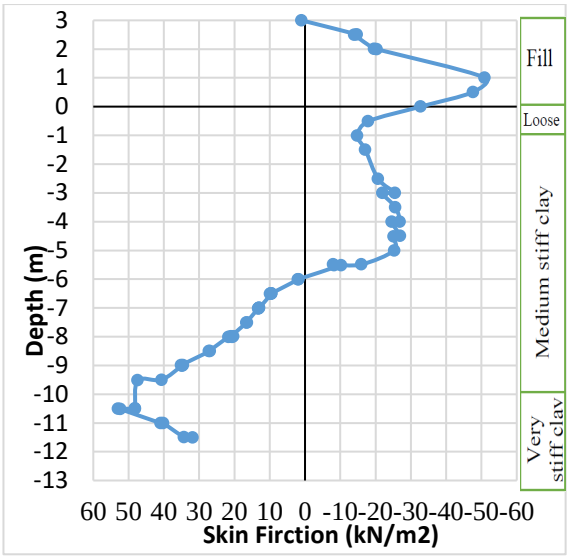

Fig. 14 Skin stress vs. depth for a driven pile at Khor Al-Zubair.

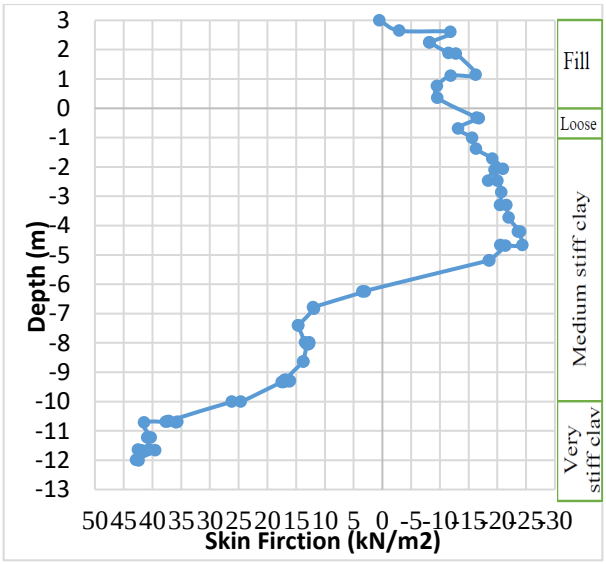

Fig. 15 Skin stress vs. depth for a bored pile at Khor Al-Zubair.

The Figures revealed maximum values of (26.8 kN/m^2) and (24.3 kN/m^2) for driven and bored piles, respectively. The neutral points are detected at (5.9 m) and (6.2 m) from the ground surface.

5.3. Shatt Al-Arab Hotel

The variation of ground settlement with time shown in Fig. 16 illustrates that a constant settlement is reached after one year.

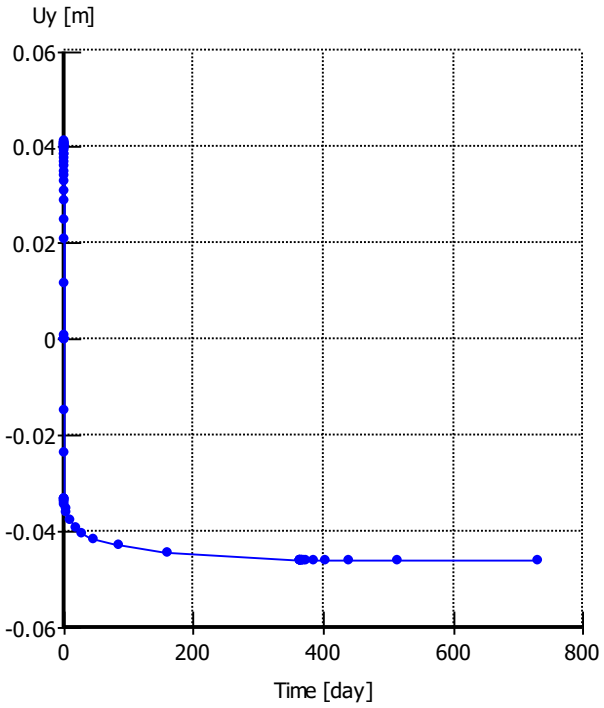

Fig. 16 Soil surface settlement vs. time at Shatt Al-Arab Hotel.

Comparisons between vertical ground displacement and single-driven and bored piles (after 365 days) at the Shatt Al-Arab Hotel site are shown in Figs. (17 and 18).

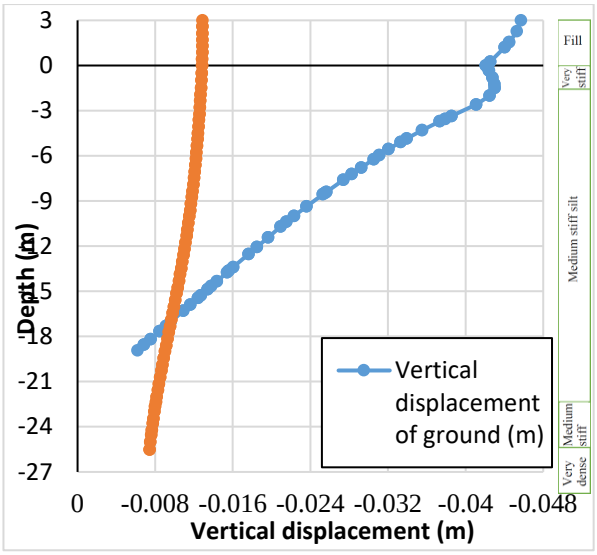

Fig. 17 Comparison between the vertical displacement of the ground and a single driven pile at Shatt Al-Arab Hotel.

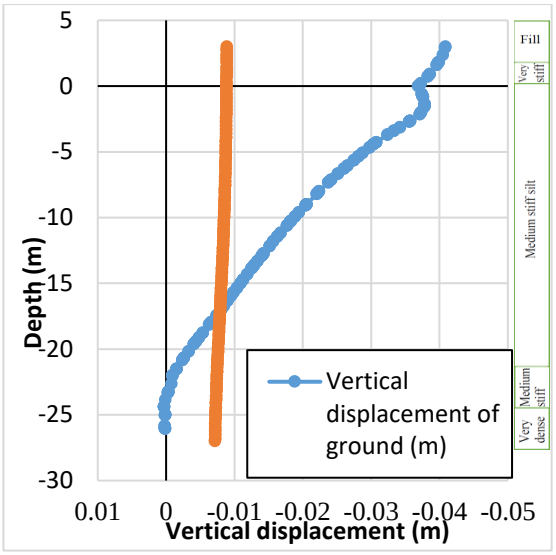

Fig. 18 Comparison between the vertical displacement of the ground and a single bored pile at Shatt Al-Arab Hotel.

The settlement values of the ground surface (after 365 days) are (0.043 m) and (0.037 m) with their counterparts of driven and bored piles of (0.013 m) and (0.009 m). The relative displacements are (0.030 m) and (0.028 m). The elastic shorting values of (0.0055 mm) and (0.0017 mm) are very clear in this site due to the increased pile lengths. The variations of skin friction along driven and bored pile shafts (after 365 days) are illustrated in Figs. (19 and 20).

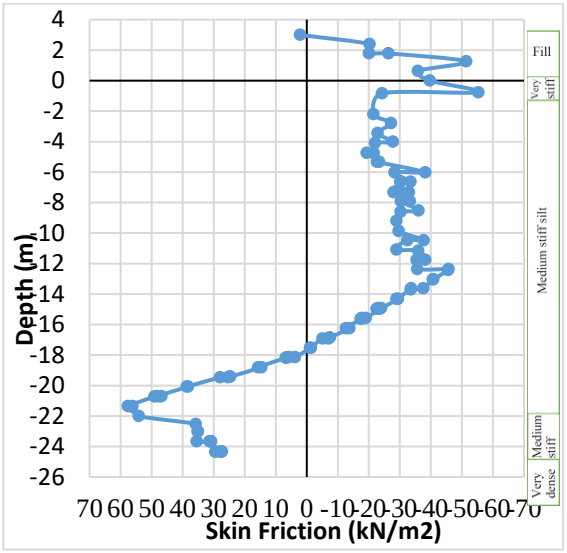

Fig. 19 Skin stress vs. depth for a driven pile at Shatt Al-Arab Hotel.

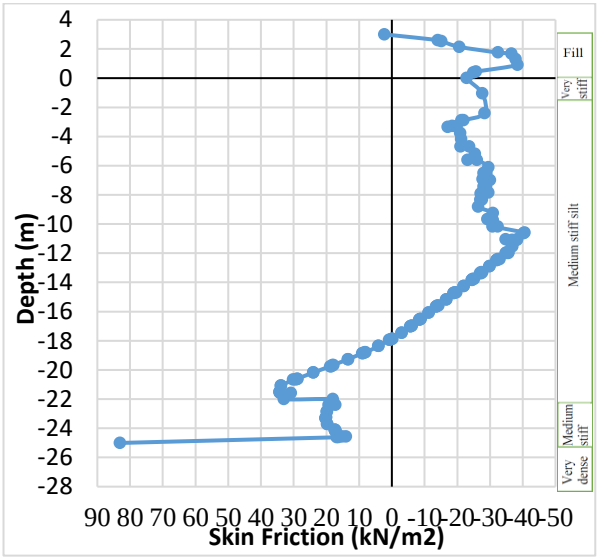

Fig. 20 Skin stress vs. depth for a bored pile at Shatt Al-Arab Hotel.

It is obvious from Figs. (19 and 20) that, the maximum negative skin friction is (45.7 kN/m^2) for the driven pile and (40.6 kN/m^2) for the bored pile. The neutral points are at (17.7 m) and (17.9 m) from the ground surface.

6. Parametric Study

An extensive parametric study is performed regarding the effects of pile cross-sectional dimensions; interface factor; and fill height, on the drag force. With constant all other factors and properties of soil and piles for three study sites (Umm Qasr Port, Khor Al-Zubair, and Shatt Al-Arab Hotel).

6.1. Effect of Pile Cross-Section Dimensions

Three sizes for each pile type are selected based on the availability in the local practice. For driven piles, the section dimensions are (0.285 m x 0.285 m); (0.35 m x 0.35 m); and (0.4 m x 0.4 m), whereas the adopted bored pile diameters are (0.6 m; 0.8 m; and 1 m).

The distributions of drag load with depth for various pile sections are shown in Figs. (21 to 26) at different locations. The results are summarized in Table 10.

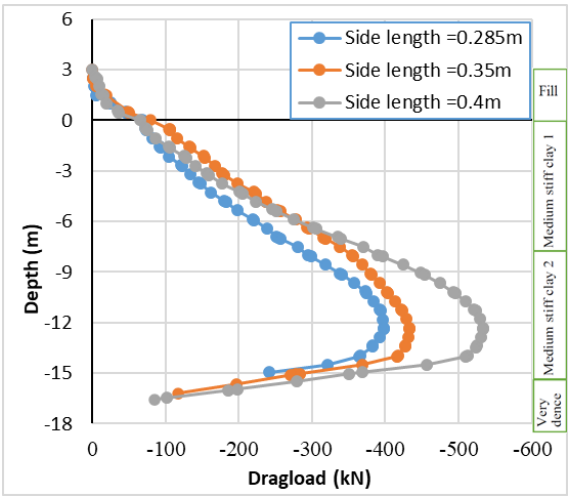

Fig. 21 Dragload vs. depth for various driven pile sections at Umm-Qasr Port.

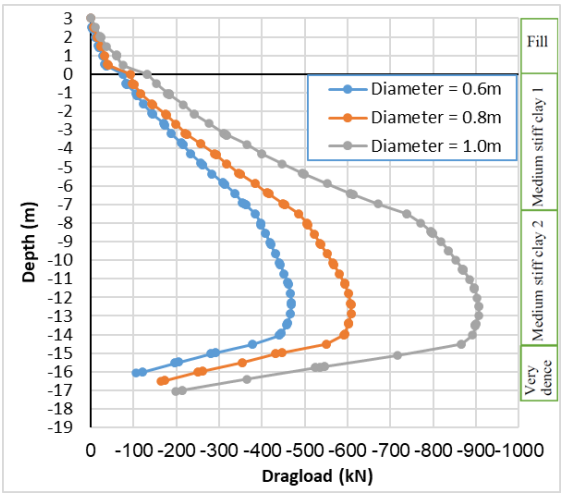

Fig. 22 Dragload vs. depth for various bored pile diameters at Umm-Qasr Port.

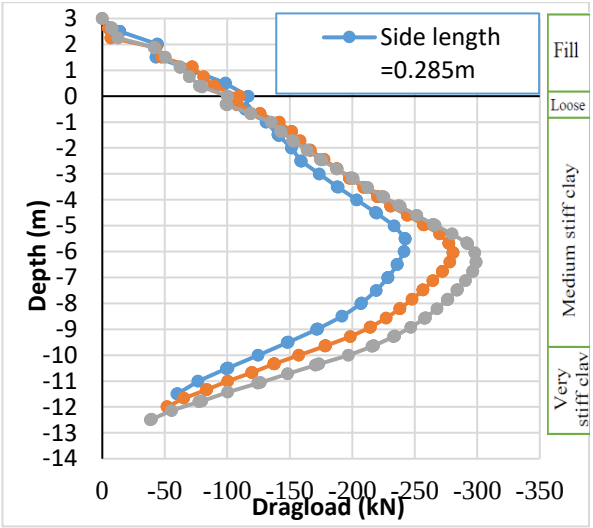

Fig. 23 Dragload vs. depth for various driven pile sections at Khor Al-Zubair.

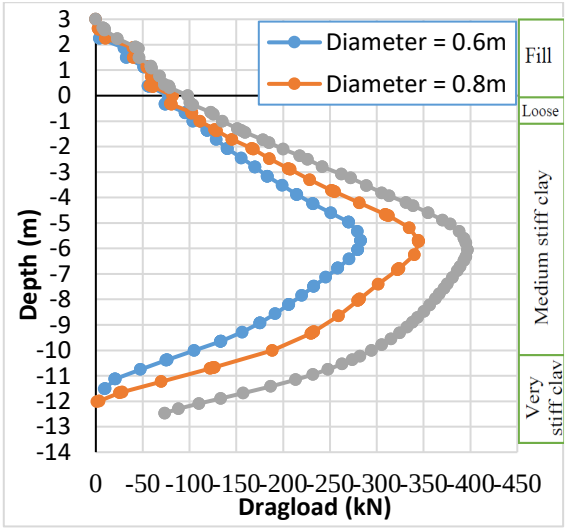

Fig. 24 Dragload vs. depth for various bored pile diameters at Khor Al-Zubair.

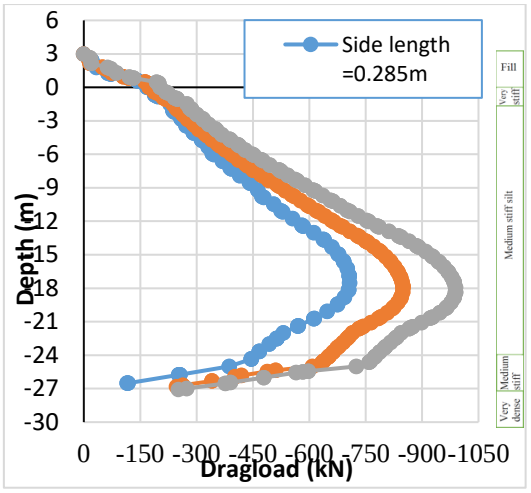

Fig. 25 Dragload vs. depth for various driven pile sections at Shatt Al-Arab Hotel.

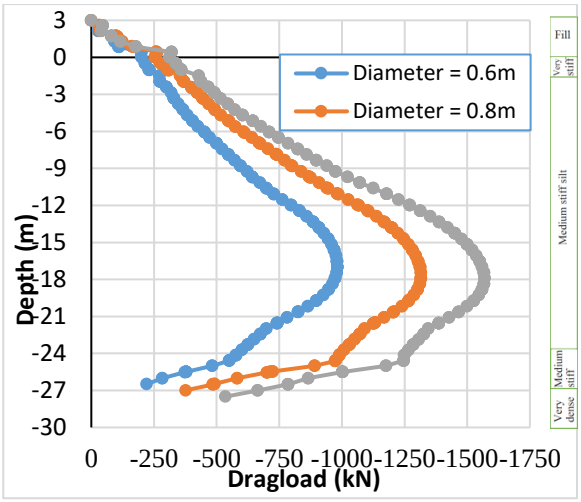

Fig. 26 Dragload vs. depth for various driven pile sections at Shatt Al-Arab Hotel.

Table 10- Comparison of maximum drag load values and neutral point depths for various pile sections.

Site		Side length of driven pile (m)			Diameter of bored pile (m)		
		0.285	**0.35**	**0.4**	**0.6**	**0.8**	**1.0**
Umm-Qasr Port	Maximum drag load (kN)	397	433	533	469	608	906
	Depth of neutral point (m)	12.0	12.6	12.4	12.4	12.9	12.5
Khor Al-Zubair	Maximum dragload (kN)	243	281	299	283	345	397
	Depth of neutral point (m)	5.5	6.0	6.4	5.7	6.2	6.0
Shatt Al-Arab Hotel	Maximum drag load (kN)	708	849	989	982	1317	1568
	Depth of neutral point (m)	17.7	17.9	18.0	17.0	17.9	17.9

Increasing pile section width by (40.4%) for driven piles, results in increasing the drag force by (23% - 39.7). Increasing pile diameter by (66.7%) for bored piles, increases the drag force by (40.3% - 93.2%).

6.2. Effect of Interface

The interface effect is studied through the interface reduction factor (R_{inter}). Four values are adopted (0.3; 0.5; 0.7; and 0.9). The variations of drag load along a driven pile shaft for different interface factors are shown in Figs. (27 to 29). The results are summarized in Table 11.

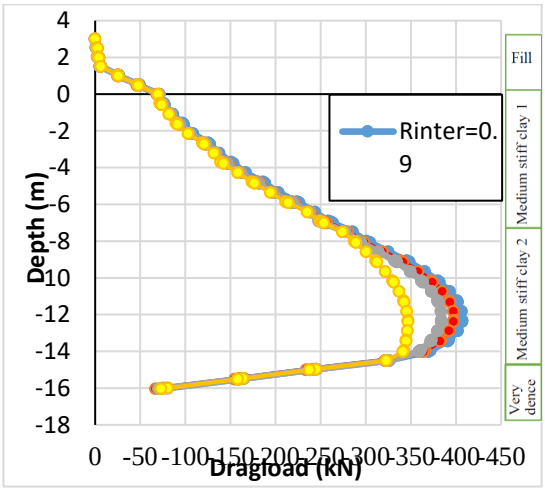

Fig. 27 Dragload vs. depth for various interface factors (driven pile at Umm-Qasr Port)

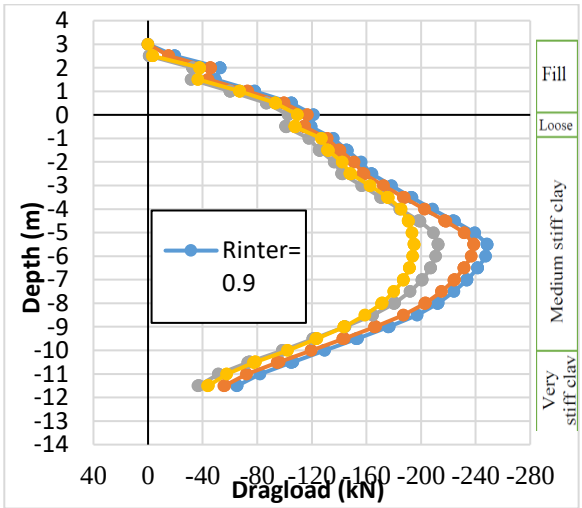

Fig. 28 Dragload vs. depth for various interface factors (driven pile at Khor Al-Zubair).

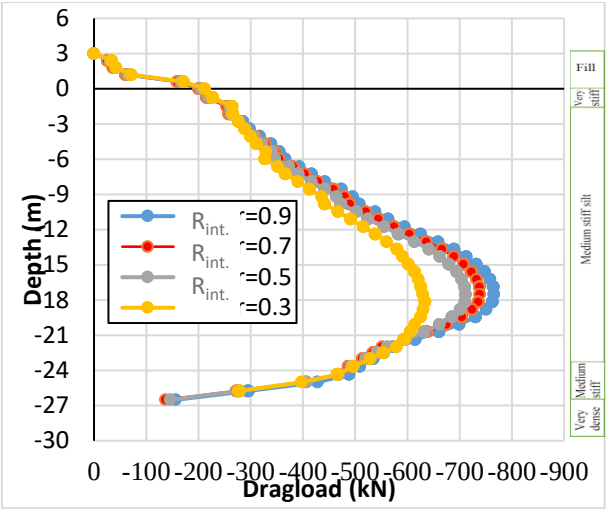

Fig. 29 Dragload vs. depth for various interface factors (driven pile at Shatt Al-Arab Hotel).

Table 11- Comparison of maximum drag load values and neutral point depths for various interface factors (0.285m x 0.285m) driven pile.

Site		R_{int}			
		0.3	0.5	0.7	0.9
Umm-Qasr Port	Maximum drag load (kN)	347	384	397	407
	Depth of neutral point (m)	12.4	12.4	12.4	12.4
Khor Al-Zubair	Maximum dragload (kN)	195	213	239	249
	Depth of neutral point (m)	5.5	5.5	5.5	5.5
Shatt Al-Arab Hotel	Maximum drag load (kN)	634	712	739	766
	Depth of neutral point (m)	18.2	17.5	17.5	17.5

Increasing the interface reduction factor by (200%) for driven piles results in increasing the drag force by (17.3% - 27.7%).

6.3. Effect of Fill Height

Three values of fill height (1 m; 2 m; and 3) are selected to study the effect of the applied consolidation stress. The variations of drag load along driven and bored pile shafts are shown in Figs. (30 to 35), at the different locations. The results are summarized in Table 12.

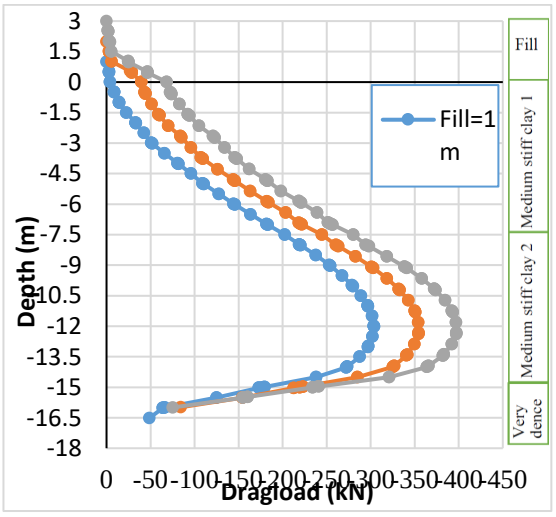

Fig. 30 Dragload vs. depth for various fill heights (driven pile at Umm-Qasr Port).

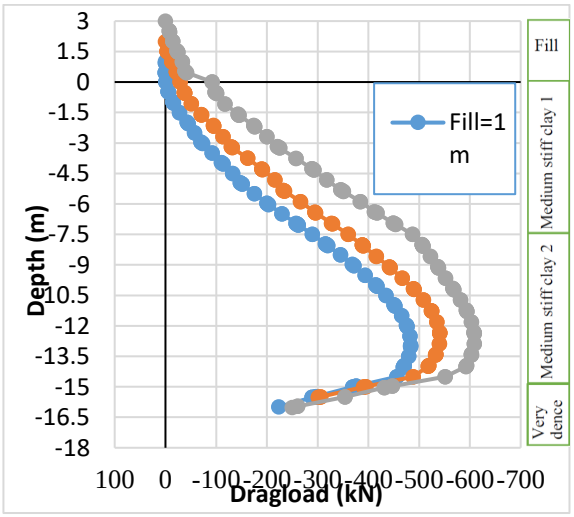

Fig. 31 Dragload vs. depth for various fill heights (bored pile at Umm-Qasr Port).

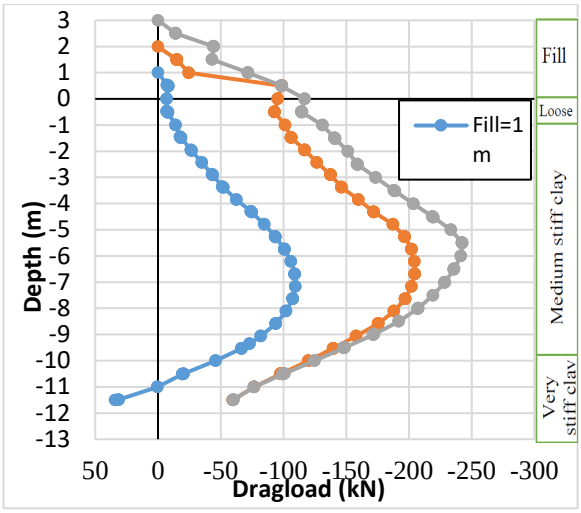

Fig. 32 Dragload vs. depth for various fill heights (driven pile at Khor Al-Zubair).

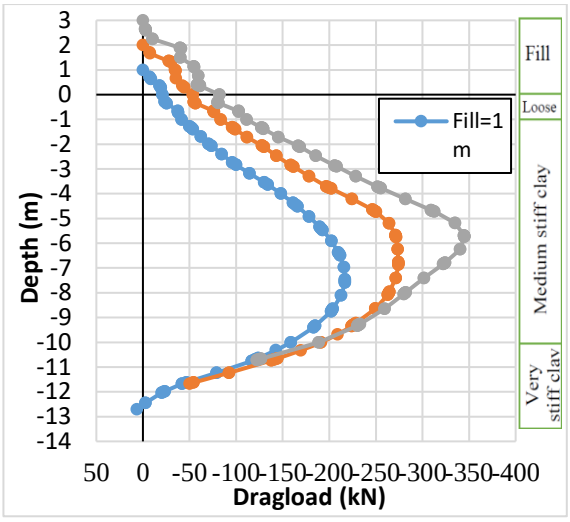

Fig. 33 Dragload vs. depth for various fill heights (bored pile at Khor Al-Zubair).

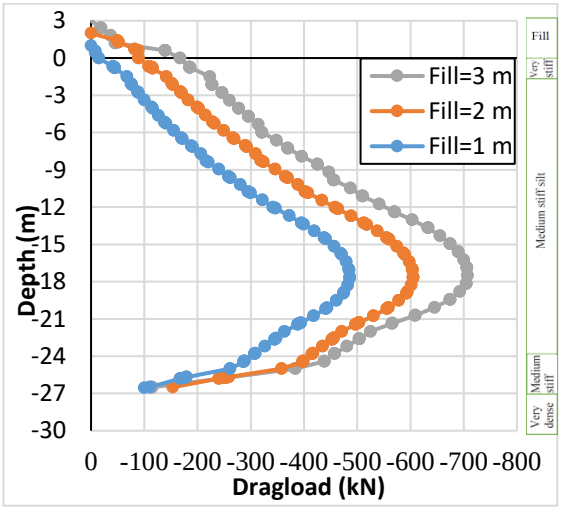

Fig. 34 Dragload vs. depth for various fill heights (driven pile at Shatt Al-Arab Hotel).

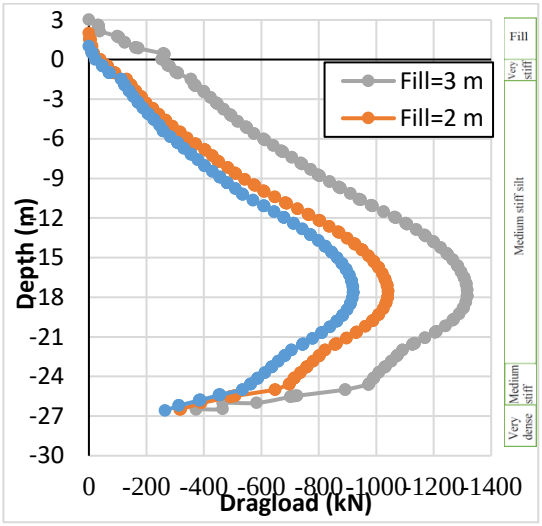

Fig. 35 Dragload vs. depth for various fill heights (bored pile at Shatt Al-Arab Hotel).

Table 12- Effect of fill height on drag load and neutral point depth for driven and bored piles.

Site		(0.285m x 0.285m) driven pile			(0.8m diameter) bored pile		
		Fill height (m)			Fill height (m)		
		1	2	3	1	2	3
Umm Qasr Port	Maximum dragload (kN)	304	354	397	483	541	608
	Depth of neutral point (m)	12	12.4	12.4	13	12.9	12.9
Khor Al-Zubair	Maximum dragload (kN)	110	205	243	217	274	345
	Depth of neutral point (m)	6.9	6.5	5.5	7.5	6.9	5.7
Shatt Al-Arab Hotel	Maximum dragload (kN)	486	605	708	920	1041	1317
	Depth of neutral point (m)	17.7	17.7	17.7	17.6	17.8	17.9

Increasing fill height by (200%) results in, increasing the drag forces by (30.6% - 120.9%) for driven piles and by (25.9% - 59.0%) for bored piles.

7. Conclusions

1. Small displacement values are necessary to activate the negative skin friction.
2. The elastic shorting for pile effect negative skin friction, due to increase relative displacement. The elastic shorting of the driven pile is more than that of the bored pile due to the less cross-sectional area of the driven pile.
3. At Khor Al-Zubair site, higher pile settlement values are obtained because piles are resting in a cohesive bearing layer.
4. The developed drag force is proportional to section dimensions, interface friction factor, and fill height (consolidation pressure). Section dimension has the maximum effect whereas, the friction factor has the minimum impact.
5. The neutral point location is not sensitive to the variation in section dimensions, interface friction factor, and fill height.

References

Kouretzis, G. (2018), "Fundamentals of Geotechnical Engineering and their Applications", The University of Newcastle, Australia.

Bowles, J. (1997), “Foundation Analysis and Design” The McGraw-Hill Companies Corp, New York, St. Louise, Fifth Edition, (1168 pp).

Zhang, J.W., Wang, Z.L. and Qiao, D.Q. (2014), "Model Test on Negative Skin Friction for Super-Long Pile Under Surcharge Load Considering Time Effect", Applied Mechanics and Materials, Vol. 470, pp. (1105-1108), Trans Tech Publications, Switzerland.

Abd El-Naiem, M.A.,Towfeek, A.R. and Hegazy, O.M.M. (2015), "Investigation of the Distribution of Skin Friction on Single Pile Constructed In Natural Soft Clay Soil Treated With Stone Columns", IJEDR, Vol.3, Issue 3, pp. (1-10).

Drbe, O., Sadrekarimi, A., El Naggar, M.H. and Sangiuliano,T. (2016), "Modelling of Negative Skin Friction on Driven Piles", GeoVancouver, pp.(1-7).

Siegel, T.C. and Lucarelli, A. (2017), "Theory and Modelling of Negative Skin Friction on a Pile in Soil", The Journal of the Deep Foundations Institute, pp.(1-8), Taylor & Francis.

Dey, A. and Koch, M.C. (2017), "Numerical Study of the Effect of Pile Driving on the Position of a Neutral Plane", American Society of Civil Engineers, Geotechnical Frontiers GSP 279, pp. (101-111).

Smith I. and Griffiths D. (2004), “Programming the Finite Element Method”, John Wily and Sons, Inc. London New York, Fourth Edition, (646 pp).

Brinkgreve, R.B.J. (2002), "PLAXIS", Delft University of Technology @ Plaxis b.v. The Netherlands.

Kiprotich,N. (2015), "Modelling of Negative Skin Friction on Bored Piles in Clay", M.Sc. Thesis, Department of Civil and Environmental Engineering, Chalmers University of Technology, Goteborg, Sweden.

Belinchon, P., Sørensen, K. K. and Christensen, R. (2016), "A Case Study of the Interaction Between a Pile and Soft Soil Focusing on Negative Skin Friction Using Finite Element Analysis", Proceedings of the 17th Nordic Geotechnical Meeting Challenges in Nordic Geotechnic, pp.(513-522),NGM Reykjavik.

Fugro Middle East (2017), “Geotechnical Factual Report, Umm Qasr Yard 5 Terminal”.

Petrolinvest (2015), "Geotechnical / Geophysical Investigation Report for Common Seawater Supply Project in Khour Al-Zubair".

The University of Basrah, Engineering Consulting Bureau (2012), “Soil Investigation Report for Shatt Al-Arab Hotel”, Report No.: 44R/SI/2012.

ACI Committee 318 (2014), “Building Code Requirements for Structural Concrete”, First Printing, September 2014, ISBN: 978-0-87031-930-3.